MATHEMATICAL MODELING AND NUMERICAL SOLUTION OF 3D ATMOSPHERIC BOUNDARY LAYER

L. Beneš, K. Kozel
Department of Technical Mathematics, CTU of Prague, CZ-12135
Z. Jaňour
Institute of Thermomechanics, Academy of Science, Prague, CZ-12135
I. Sládek
Department of Mathematics, CTU of Prague, CZ-12135

A mathematical and numerical investigation of the flow over 2D and 3D hilly terrain in the atmospheric boundary layer (ABL) is presented including comparison with an experiment. Mathematical model is based upon the RANS equations for an incompressible flow with an algebraic turbulence closure and given boundary conditions. Also additional transport equations for concentration and potential temperature have been considered. The artificial compressibility method with conjunction of finite volume method and the explicit Runge — Kutta multistage scheme is used for numerical analysis.

Nomenclature

L — Characteristic length; U — Characteristic velocity; h — Height of hill; $(u, v, w)^T$ — Non-dimensional velocity vector; p — Non-dimensional pressure; x, y, z — Non-dimensional space variables; t — Non-dimensional time; Re — Laminar Reynolds number; Re_T — Turbulent Reynolds number; K — Turbulent diffusion coefficient; Θ — Potential temperature; C — Concentration of passive pollutant; $_x$, $_y$, $_z$ — Space derivatives; $_t$ — Time derivative; i, j, k — Indexes in the x-, y- and z-directions; n — Discrete time level; $\Delta x, \Delta y, \Delta z$ — Space and time increments

1. Introduction

The lowest part of the atmosphere is often called the atmospheric boundary layer (ABL). Its thickness depends on various conditions and ranges from several hundreds of meters to approximately two kilometers. The ABL is significantly influenced by the roughness of the earth's ground, geostrophic wind and mainly by the vertical temperature gradient which is associated with the atmospheric thermal stratification.

The ABL has a very close relation to a human activity. Prediction of wind field over complex terrain plays a dominant role in many engineering applications such as evaluation of environmental impact by pollutant dispersion, sitting of wind mills and airports *etc.* Practically, an infinite number of situations are possible even for the wind flow over a single hill due to varieties of hill geometry and approaching flow conditions.

Nevertheless, there are still gaps in the detailed understanding of the turbulent flow including flow separation. Because of the difficulties and high cost of experiments associated with the investigation of all possible situations, a more reliable numerical method is desired to predict the complex wind flow over such hilly terrain.

2. Mathematical model

We suppose turbulent, viscous, incompressible and stationary flow under stably ($\frac{\partial\Theta}{\partial z} > 0$) or neutrally ($\frac{\partial\Theta}{\partial z} = 0$) stratified atmosphere. The buoyancy force is neglected.

3. Governing equations

Mathematical model is given by the Reynolds averaged Navier-Stokes equations in conservative, dimensionless and vector form in the physical domain Ω (Kozel [1], Jaňour [2])

$$F_x + G_y + H_z = (K \cdot R)_x + (K \cdot S)_y + (K \cdot T)_z \tag{1}$$

The artificial compressibility method is used for numerical analysis

$$W_t + F_x + G_y + H_z = (K \cdot R)_x + (K \cdot S)_y + (K \cdot T)_z \tag{2}$$

We solve system (2) in Ω under stationary boundary conditions for $t \to \infty$ (t is an artificial time) to obtain expected steady-state solution W,

$$\begin{aligned}
W &= \|p, u, v, w, \Theta, C\|^T \\
F &= \|u, u^2 + p, uv, uw, u\Theta, uC\|^T \\
G &= \|v, vu, v^2 + p, vw, v\Theta, vC\|^T \\
H &= \|w, wu, wv, w^2 + p, w\Theta, wC\|^T \\
R &= \|0, u_x, v_x, w_x, \frac{1}{\sigma_\Theta}\Theta_x, \frac{1}{\sigma_C}C_x\|^T \\
S &= \|0, u_y, v_y, w_y, \frac{1}{\sigma_\Theta}\Theta_y, \frac{1}{\sigma_C}C_y\|^T \\
T &= \|0, u_z, v_z, w_z, \frac{1}{\sigma_\Theta}\Theta_z, \frac{1}{\sigma_C}C_z\|^T
\end{aligned}$$

where F, G, H denote inviscid fluxes and R, S, T viscous ones, σ_Θ, σ_C represent Prandtl's numbers for potential temperature Θ and concentration C of passive pollutant, p refers to the pressure and $\|u,\ v,\ w\,\|^T$ denotes the velocity vector, K is the diffusivity coefficient, see equation (3).

4. Turbulence model

Closure of the system of governing equations (2) is achieved by a simple algebraic turbulence model which takes the form (Jaňour [2], Bednář [3], Jaňour [4])

$$\nu_T = G \cdot l^2 \cdot \sqrt{u_z^2 + v_z^2}$$

where ν_T is the turbulent viscosity, G the stability parameter and l refers to the Blackadar's mixing length computed from

$$l = \frac{k(z + z_0)}{1 + \frac{k(z+z_0)}{l_\infty}}$$

where k is the von Karman constant, z_0 the roughness length and l_∞ denotes the mixing length for $z \to \infty$. The diffusion coefficient K is taken as

$$K = \frac{1}{\mathrm{Re}} + \frac{1}{\mathrm{Re}_T} \tag{3}$$

where Re is laminar, Re_T is turbulent Reynolds number respectively.

5. Initial and boundary conditions

The following stationary initial and boundary conditions are considered (Jaňour [2], Bednář [3])

- initial conditions in domain Ω
  - — p, u, v, w, Θ, C given
- boundary conditions on $\partial\Omega$
  - — inlet: p given or $p_x = 0$, u, v, w, Θ, C prescribed from experiment or theory (Schlichting [5]), point source of C is usually assumed
  - — outlet: p given, $u_x = v_x = w_x = 0, \Theta_x = 0, C_x = 0$
  - — bottom face (ground): $u = v = w = 0$ as no–slip wall b.c., $\Theta = 0, \frac{\partial C}{\partial n} = 0$
  - — top face: p given, u given or $u_z = 0$, v given or $v_z = 0$, w given or $w_z = 0, \Theta_z = 0, C_z = 0$
  - — side faces: periodic

We expect that the solution of (2) will be steady for $t \to \infty$ and also fulfilling (1).

6. Numerical model

Finite volume method (cell-centered) together with the multi–stage explicit Runge— Kutta time integration scheme is used to solve (2) (Kozel [1], Hirsch [6]). After integration of (2) over control cell Ω_{ijk} we obtain

$$\iiint_{\Omega_{ijk}} W_t \, dV = -\iiint_{\Omega_{ijk}} \Big[(F - K \cdot R)_x + (G - K \cdot S)_y + (H - K \cdot T)_z\Big] \, dV$$

and using the Divergence theorem

$$W_t\Big|_{ijk} = -\frac{1}{\mu_{ijk}} \oiint_{\partial\Omega_{ijk}} \Big[(F - K \cdot R)\, dS_1 + (G - K \cdot S)\, dS_2 + (H - K \cdot T)\, dS_3\Big] \tag{4}$$

where $W_t\Big|_{ijk}$ is the mean value of W over cell Ω_{ijk} and $\mu_{ijk} = \iiint_{\Omega_{ijk}} dV$ is volume of control cell.
The central differences are used for space discretization in order to obtain semi–discrete system of equations.

$$W_t\Big|_{ijk}(t) = \mathbf{L}W_{ijk}(t) \tag{5}$$

where $\mathbf{L}W_{ijk}$ denotes approximation of the right-hand side of (4)

$$\mathbf{L}W_{ijk} = -\frac{1}{\mu_{ijk}} \sum_{l=1}^{6} \Big[(\tilde{F}_l - K_l \cdot \tilde{R}_l)\, \Delta S_1^l + (\tilde{G}_l - K_l \cdot \tilde{S}_l)\, \Delta S_2^l + (\tilde{H}_l - K_l \cdot \tilde{T}_l)\, \Delta S_3^l\Big]$$

where all symbols denoted with subscript $_l$ refer to the l–th cell face of Ω_{ijk} and $(\Delta S_1^l, \Delta S_2^l, \Delta S_3^l)$ represents the l–th outer normal vector.
Finally, the (3)–stage explicit Runge— Kutta time integration scheme is applied to system (5)

$$\begin{aligned} W_{ijk}^{(0)} &= W_{ijk}^{n} \\ W_{ijk}^{(l+1)} &= W_{ijk}^{(0)} - \alpha_l \cdot \Delta t \cdot \mathbf{B}W_{ijk}^{(l)}, \ l = 0, \ldots, 2 \\ W_{ijk}^{n+1} &= W_{ijk}^{(3)} \end{aligned}$$

where $\alpha_1 = 1/2, \alpha_2 = 1/2, \alpha_3 = 1$. The operator $\mathbf{B}W_{ijk}^{(l)}$ defines a steady residual in the l–th time level for each control cell Ω_{ijk}

$$\mathbf{B}W_{ijk}^{(l)} = \mathbf{L}W_{ijk}^{(l)} + \mathbf{D}W_{ijk}^{(0)}$$

where $\mathbf{L}W_{ijk}$ corresponds to operator resulting from the space discretization of system (4) and the second term $\mathbf{D}W_{ijk}$ represents the artificial diffusion term of the 2^{nd} or 4^{th} order for which it has the following form

$$\mathbf{D}W_{ijk} = \varepsilon_x \Delta x^4 W_{xxxx}\Big|_{ijk} + \varepsilon_y \Delta y^4 W_{yyyy}\Big|_{ijk} + \varepsilon_z \Delta z^4 W_{zzzz}\Big|_{ijk}$$

The stability criterion for regular orthogonal mesh is applied by

$$\Delta t \leq \min_{\Omega_{ijk}} \frac{CFL}{\frac{\varrho_A}{\Delta x} + \frac{\varrho_B}{\Delta y} + \frac{\varrho_C}{\Delta z} + 2 \cdot K \left(\frac{1}{\Delta x^2} + \frac{1}{\Delta y^2} + \frac{1}{\Delta z^2}\right)}$$

and the rate of convergence is examined using residual L_2 norm

$$\|\mathrm{Re}\mathbf{z}\, W^n\|_{L_2} = \mathrm{const} \cdot \left(\sum_{i,j,k} (\mathbf{B}W_{ijk}^n)^2\right)^{\frac{1}{2}}.$$

7. Some numerical results

An IBM SP2 machine in the super-computing center of the Czech Technical University of Prague and workstations of the Dept. of Technical Mathematics, CTU have been used for all computations.

Comparison with 2D experiment

Fully developed channel flow over 2D polynomial–shaped hill mounted on a flat plate was chosen as a test–case. The results from experimental measurement (Almeida [7]) and reference numerical simulations with $k-\varepsilon$ turbulence model (Davroux [8]) have been used for comparison with our computations performed on three different grids, see Fig. 1–4. Notice that both sets of results are also available in the ERCOFTAC database (see [9]).

The channel height is 170 mm and the hill height is $h = 28$ mm (~ 16 % hill). Mean centerline velocity, U_0, and hill height, h, have been used to nondimensionalize the velocity profiles.

Main flow parameters are:

— mean centerline velocity $U_0 = 2.147\,\mathrm{m/s}$

— water kinematic viscosity $\nu = 1 \cdot 10^{-6}\,\mathrm{m^2/s}$

— Reynolds number $\mathrm{Re} = U_0 \cdot h/\nu = 6 \cdot 10^4$

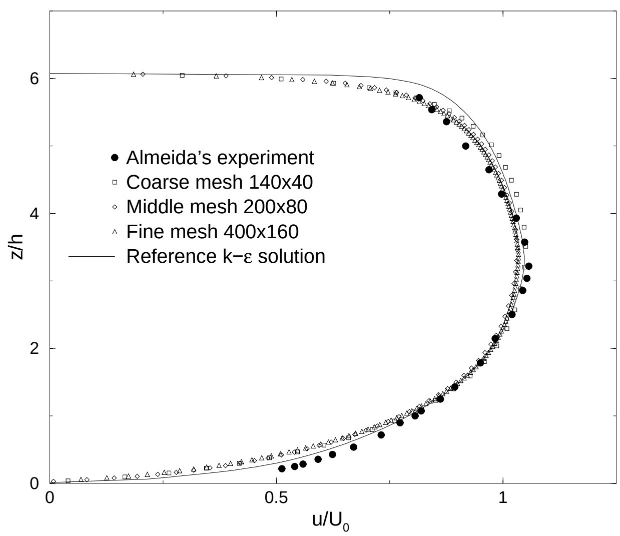

Fig. 1: Profiles of streamwise velocity component at the position 50 mm before hill summit.

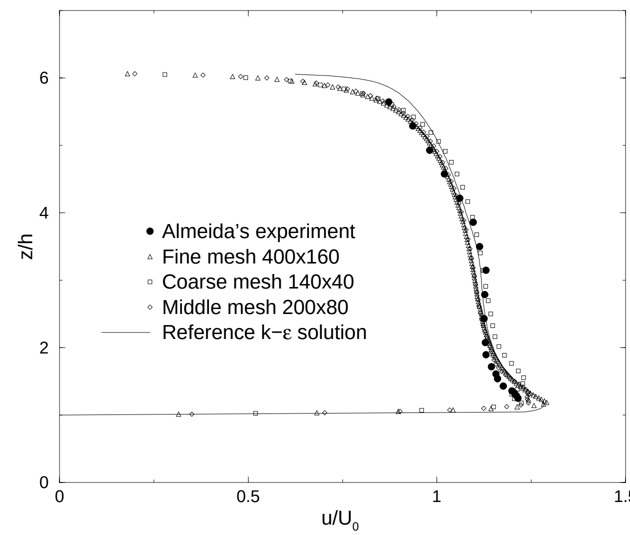

Fig. 2: Profiles of streamwise velocity component at the hill summit.

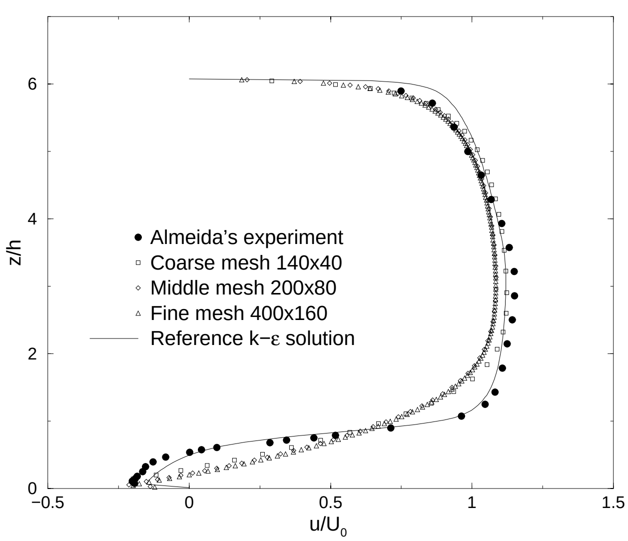

Fig. 3: Profiles of streamwise velocity component at the position 50 mm after hill summit.

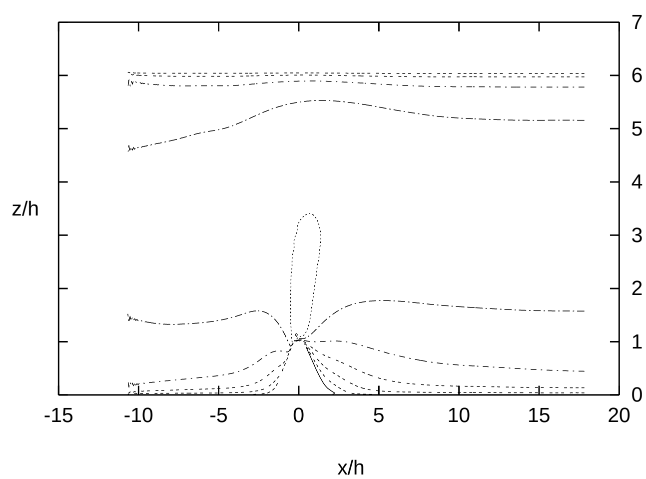

Fig. 4: Streamwise cut over the domain and over hill, isolines of velocity magnitude.

Some 3D results

We present some 3D results (Kozel *et. al.* [10], [11], [12]) from computations over a single hill configuration, see Fig. 5–8.

Dimensions of the physical domain are: 8x4x1 km for length, width and height respectively and 10 % hill is assumed. The characteristic free–stream velocity is $U = 1$ m/s and characteristic length $L = 1$ km leading to the Reynolds number $\mathrm{Re} = 7 \cdot 10^7$, the uniform velocity profile is imposed at the inlet and stably stratified atmosphere is supposed $\frac{\partial \Theta}{\partial z} = 0.005$ K/m.

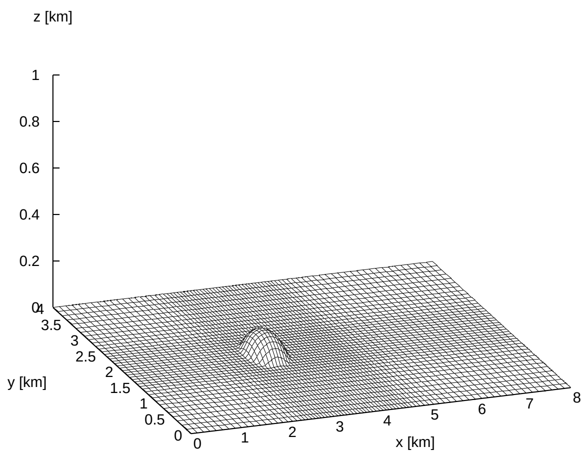

Fig. 5: Computational domain with a single hill configuration.

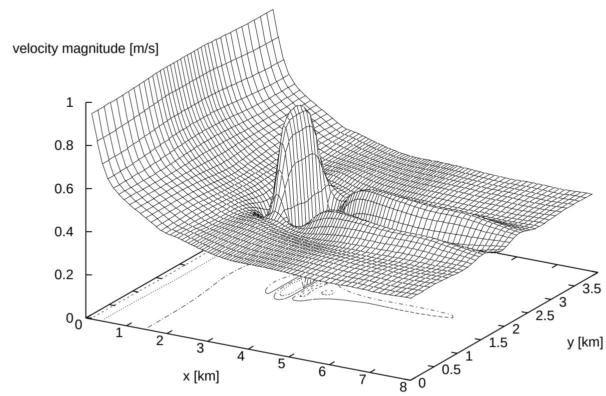

Fig. 6: Single hill configuration, isolines of velocity magnitude on xy-cutplane over the domain at constant height z=20 m.

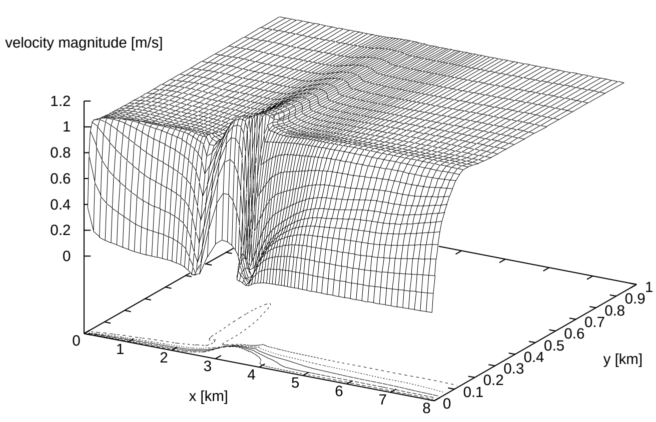

Fig. 7: Single hill configuration, isolines of velocity magnitude on streamwise xz-cutplane over the domain and over hill.

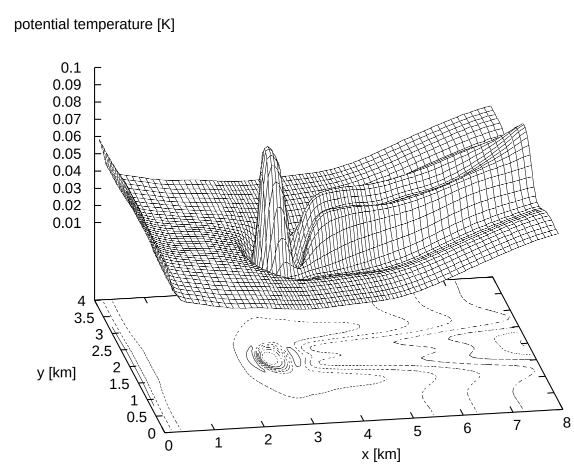

Fig. 8: Single hill configuration, isolines of potential temperature on xy-cutplane over the domain at constant height z=20 m.

We also present some 3D results obtained from simulations over a complex hilly terrain, see Fig. 9–10, and also double hill configuration, see Fig. 11–12. The Reynolds number in these cases is $\mathrm{Re} = 1 \cdot 10^8$.

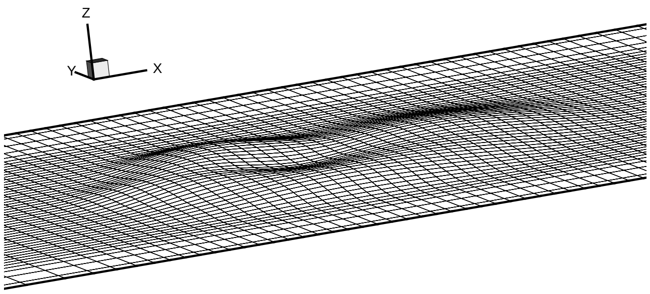

Fig. 9: Part of computational domain showing a complex 3D hilly terrain.

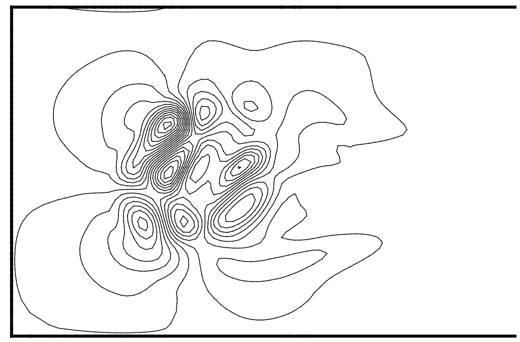

Fig. 10: Isolines of velocity on the ground.

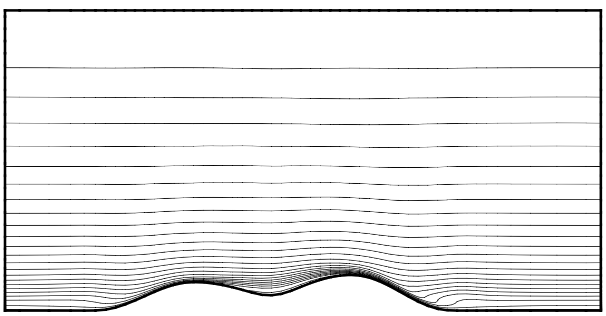

Fig. 11: Double–hill configuration, streamwise cutplane over the domain and isolines of velocity.

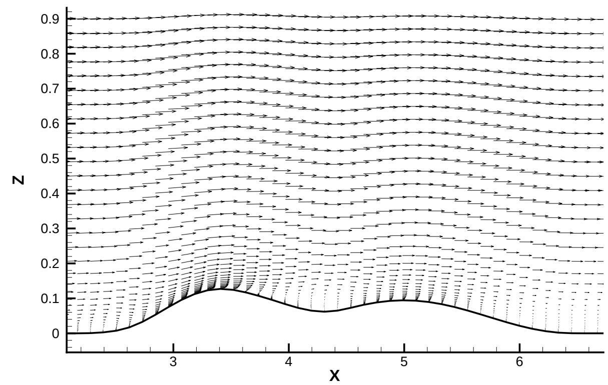

Fig. 12: Double–hill configuration, streamwise cutplane over the domain and vector field.

8. Summary and Conclusion

• A number of numerical simulations with high Reynolds numbers have been performed for the flow over three–dimensional single hill or system of hills using different grids and various initial and boundary conditions have been tested. The curved shapes of the geometry were fitted by means of the Cartesian non–orthogonal grids.

• The calculations have shown that the flow field is sensitive to the specification of the inflow conditions. Transport equations for the potential temperature and concentration of passive pollutant were also solved to obtain temperature and concentration fields above 3D–topography.

• The calculations have confirmed that the artificial diffusion term plays an important role in the numerical algorithm. It does inhibit various small oscillations arising in the flow field. These oscillations appear due to the central differencing scheme and low level of artificial viscosity.

• Because of the absence of some real experiment it seems to be very difficult to carry out a quantitative comparison between measured and computed data. Therefore, our results have been compared with the experimental data (Almeida [7]) and the reference numerical data (Davroux [8]) obtained from a simplified test–case configuration of fully developed channel flow over a 2D hill. A good agreement has been found for velocity profiles up to hill summit streamwise position. However, the recirculation area behind a hill has shown some deviations of velocity profiles from target values most probably due to the simplicity of turbulence model. Additional simulations and comparisons with other data sets are required.

• Thus, the implementation of a more complex turbulence model (Jaňour [4]) suitable for the ABL seems to be an important point of mathematical model development as well as the application of higher order schemes or implicit schemes to accelerate the computations and to increase the numerical accuracy. Also an employment of some orthogonal computational grids would be valuable in order to test the effect of grid orthogonality. Notice, that the buoyancy forces plays one of the key role in the ABL and hence they should be incorporated into the physical model when thermal stratification is assumed.

Acknowledgements

This work was supported by grants 101/98/K001 and 205/01/1120 of Grant Agency of Czech Republic, COST OC. 715.70 and Research Plan MSM 210000003. Thanks are also extended to the super-computing center of the CTU of Prague.

References

[1] Dvořák R., Kozel K.: Mathematical Modeling in Aerodynamics, Prague, 1996, (in Czech).

[2] Jaňour Z.: Mathematical Modeling of Pollution Dispersion in the Atmosphere, Institute of Thermomechanics CAS, Prague 1995, (in Czech).

[3] Bednář J., Zikmund O.: Physics of the Atmospheric Boundary Layer, Academia, Prague 1985, (in Czech).

[4] Jaňour Z.: Mathematical Modeling of the Atmospheric Boundary Layer Flow in Urban Area, Institute of Thermomechanics CAS, Prague 2000, (in Czech).

[5] Schlichting H.: Boundary–Layer Theory, Mc.Graw–Hill, Hamburg, 1979.

[6] Hirsch Ch.: Numerical Computation of External and Internal Flows, Vol. 1,2, John Wiley & Sons, N. Y. 1991.

[7] Almeida G.P., Durao D.F.G., Heitor M.V.: Wake Flows Behind Two Dimensional Model Hills, Exp. Thermal and Fluid Science, 7, P. 87, 1992.

[8] Davroux A., Hoa C., Laurence D.: Flow Over a 2D Hill – Reference Solutions for k-ε and Second Moment Closure Turbulence Models, Workshop, Karlsruhe 1995.

[9] WWW site of ERCOFTAC database: http://cfd.me.umist.ac.uk/ .

[10] Beneš L., Jaňour Z., Kozel K., Sládek I.: Mathematical Modeling and Numerical Solution of Atmospheric Boundary Layer, In *Euler and Navier — Stokes Equations'98*, Prague, 1998.

[11] Beneš L., Kozel K., Sládek I.: Numerical Solution of Atmospheric boundary layer flows, In *GAMM'99*, Metz, 1999.

[12] Beneš L., Bodnár T., Fraunie Ph., Jaňour Z., Kozel K., Sládek I.: Solution of Atmospheric Boundary Layer Flows With Transport of Pollutants, In *TRANSFER'99*, Brno, 1999.